academicJournals

Vol. 12(19), pp. 188-199, 15 November, 2017
DOI: 10.5897/SRE2017.6543
Article Number: D894FFB55249
ISSN 1992-2248

http://www.academicjournals.org/SRE

Scientific Research and Essays

Full Length Research Paper

Time step-size on simulation of tree-induced capillary potential in unsaturated soils

Mu'azu Mohammed Abdullahi

Civil Engineering Department, Jubail University College, Royal Commission of Jubail and Yanbu, Jubail Industrial City, Kingdom of Saudi Arabia.

Received 8 October, 2017; Accepted 1 November, 2017

Unreliability in the assumption of soil properties, selection of elapse time, choice of time step size and atmospheric variables causes most inconsistencies in the simulation results. Therefore, time step size studied was based on root water up-take on a single Lime tree on a Boulder Clay. The effects of ¼, ½ and 1 day time step sizes on generated capillary potential at 0.0 m, 1.4 m and 3.0 m from the lime tree for elapse time of 30, 90, 190 and 270 days elapsed time were studied. A straightforward sink term for root water uptake was used and combined with two-dimensional axi-symmetric governing equation for unsaturated soil. The simulated capillary potential was directly proportional to the elapsed time. The time step sizes studied were found to give the same generated capillary potentials at same spacial distances. The idea was to investigate the generated capillary potentials at ¼, ½ and 1 days time steps sizes at a same spatial distance from the Lime tree on a Boulder Clay should be the same. Consequently, the difference in the results generated with the three initial time step sizes were far less than ±5%, which is satisfactory.

Key words: Unsaturated soil, boundary condition, capillary potential, spatial discretization, time discretization.

INTRODUCTION

A sink term for root water uptake was derived by Rees and Ali (2006) and combined with two-dimensional axi-symmetric equation for unsaturated soil. A couple of researchers have investigated root water uptake in both coupled and uncoupled approaches to ground deformation (Fredlund and Hung, 2001; Navarro et al., 2009; Fatahi et al., 2010, 2009). The root water uptake could be modelled as 1-D, 2-D and 3-D while according to Bechmann et al. (2014), the non-uniformity of root hydraulic properties as important component needed to be accounted for in complex 3-D root water uptake model analysis. Daly et al. (2017) quantified root water uptake in the soil using X-ray computed tomography and image-based modeling and noticed that the spatially averaged models worked well in comparison to the image-based models with <2% difference. A solution of water uptake by plant roots can be dealt with in two main ways (Nyambayo and Potts, 2010; Thomas and Rees, 1991). The first approach considers that water flow to a single root, called 'microscopic' approach, while the second method considers the root systems analyzed as a single unit called 'macroscopic'. The second model is widely

E-mail: muazum@ucj.edu.sa.

used and allows interaction of transpiration process, inclusion of a volumetric sink term in Richard's equation to accommodate water-uptake (Feddes et al., 1976; Mathur and Rao, 1999). Kumar et al. (2014) stipulated that the correctness of water uptake forecast by plants depend on mathematical representation used and are obtainable in the form of linear, nonlinear, and exponential. The capability of roots to take up water depends on both root distribution and root water uptake effectivity; the previous will be experimentally measured, at the same time the latter is particularly complex to assess (Li et al., 2013).

Liao et al. (2016) proposed inverse method for estimation of root water uptake which applies only if the following conditions are satisfied: the time interval is between 5-17 days, the time step at the range of 1000-10000 and the rate of soil surface evaporation is ≤ 0.6 mm/d. The developed formulation to predict the changes in capillary potential and the numerical model can be used to investigate the effects of a wide range of soils, trees and atmospheric parameters on unsaturated soils. If the solution converges and tends to zero, then the system is considered stable. The stress-deformation model was validated by Mu'azu et al. (2011) and primary data used in validating the model was reported by Biddle (1998). Martin et al. (2015) accordingly carried out modeling of two different water uptake approaches for mono- and mixed-species forest stands and discovered no single strategy performs best regarding substantiation of data sets, Martin et al. (2015) postulated that a better may be accomplished when measurements of root length, densities and water uptake rates of fine roots are integrated. Knowledge of the relationship between soil and plant water is limited due to lack of experimental methods to measure water fluxes in soil and plants, according to Mohsen et al. (2014). However, root water uptake was higher in the proximal parts of lateral roots and decreased toward the distal parts (Mohsen et al., 2014).

According to Saroj and Sandeep (2011), the impact of the time step is not so adequately studied and is poorly understood (Saroj and Sandeep, 2011). Dai et al. (2010) is a stepwise inverse method with capacities to quantify permeabilities at various spatial scales, which leads to reducing the uncertainty of estimated parameters

Due to non-linear numerical stability, spurious numerical oscillations may occur with large time step size (Teixeira et al., 2007). Root water uptake profile was estimated by the mixing model and the mechanistic model with later calibrated with isotopes gave better results and the use of the mixing model is not recommended unless appropriate constraints are applied (Tsutomu et al 2017).

The effect of lateral distances and elapse time on the generated capillary potential is relevant. This analysis elaborated the space and time dependency of capillary potential due to root water-uptake. The main objective of the study is to investigate time step sizes, to know whether the convergence criteria have been met.

METHODOLOGY

Two theoretical approaches are used to represent moisture flow in a non-deformable soil viz, the diffusivity based formulation (Philip, 1957) and capillary potential, and is based on Richard's theoretical formulation (Richards, 1931). Alonso et al. (1987) states that Richard's formulation is preferred in practice with sinks term as shown in Equation 1:

$$C(\psi)\frac{\partial\psi}{\partial t}=\frac{\partial}{\partial r}\left[K(\psi)\frac{\partial\psi}{\partial r}\right]+\frac{\partial}{\partial z}\left[K(\psi)\frac{\partial\psi}{\partial z}\right]+\frac{\partial K(\psi)}{\partial z}+\frac{1}{r}K(\psi)\frac{\partial\psi}{\partial r}-S(\psi,r,z) \quad (1)$$

Where $K(\psi)$ is the unsaturated hydraulic conductivity, t is the time, r and z are the coordinates, θ is the volumetric moisture content and ψ is the capillary potential, $S(\psi, r, z)$ is the root water extraction function and r is the radial coordinate. The root water-uptake extraction function is the sink term $S(\psi, z, r)$ in the Equation 1. For water-uptake in two dimensional axi-symmetric form (Rees and Ali, 2006) comprising of vertical and radial components, incorporating water stress function when soil moisture is limiting is given as:

$$S(\psi,z,r)=\frac{4T}{z_r r_r}\alpha(\psi)\left(1-\frac{z}{z_r}\right)\left(1-\frac{r}{r_r}\right) \quad (2)$$

Where $\alpha(\psi)$ (dimensionless) is a prescribed function of the capillary potential referred to as water-stress function.

Finite element spatial discretization

The spatial and time variations of the unknown variable are estimated where the problem at hand requires capillary to be computed. The numerical solution is achieved by discretizing the 2-D axi-symmetric space domain and the time domain. The process of approximating a given function by using trial functions provides a useful introduction to the finite element approach (Rockey et al., 1983; Zienkiewicz and Taylor, 1989) clearly illustrate approximation by trial functions.

The numerical solution of Equation 1 was achieved via the finite element spatial discretization procedure and a finite-difference time-stepping scheme adopting particular Galerkin weighted residual approach. The parabolic shape functions and eight-node isoperimetric elements are employed (Zienkiewicz and Taylor, 1989). Equation 1 is discretized as:

$$K\psi_s+C\frac{\psi_s}{\partial t}+J+S=0 \quad (3)$$

Where:

$$K=\sum_{e=1}^{m}\int_{\Omega^e} r\left[K\frac{\partial N_s}{\partial r}\cdot\frac{\partial N_r}{\partial r}+K\frac{\partial N_s}{\partial z}\cdot\frac{\partial N_r}{\partial z}\right]\partial\Omega^e \quad (4)$$

$$C=\sum_{e=1}^{m}\int_{\Omega^e} r\left[N_r N_s C\right]\partial\Omega^e \quad (5)$$

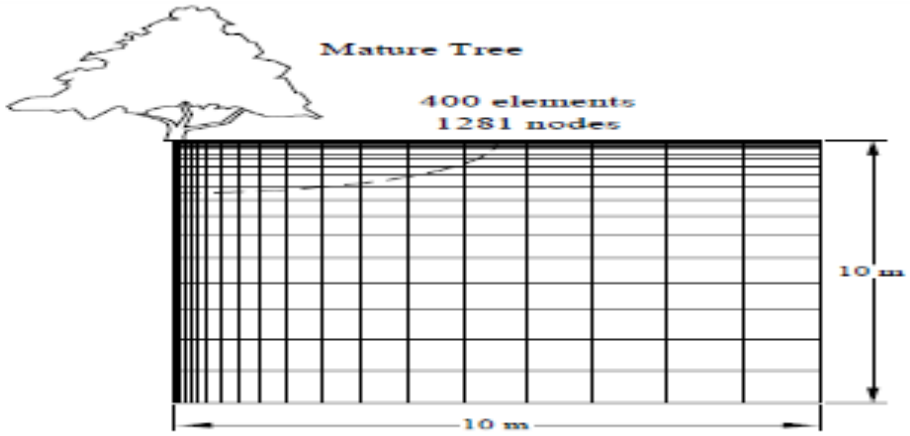

Figure 1. Finite element mesh and axi-symmetric domain (10 m × 10 m).

$$J = \sum_{e=1}^{m} \int_{\Omega^e} r\left[N_r \frac{\partial K}{\partial z} \right] \partial\Omega^e - \sum_{e=1}^{m} \int_{\Gamma^e} r\left[N_r \lambda \right] \partial\Gamma^e \quad (6)$$

$$S = \sum_{e=1}^{m} \int_{\Omega^e} r\left[N_r S(r,z) \right] \partial\Omega^e \quad (7)$$

Time discretization

The spatially discretized matrix in Equation 3 is a time discretized by the application of a fully implicit mid-interval backward difference algorithm (Neuman, 1973) and illustrated by Thomas and Rees (1991) who provided the following description as expressed in Equation 3, which may be approximated by:

$$K^{n+1/2}\psi^{n+1} + C^{n+1/2}\left[\frac{\psi^{n+1} - \psi^{n}}{\Delta t} \right] + J^{n+1/2} + S^{n+1/2} = 0 \quad (8)$$

Rearranging yields:

$$\psi^{n+1} = \left[K^{n+1/2} + \frac{C^{n+1/2}}{\Delta t} \right]^{-1} + \left[\frac{C^{n+1/2}\psi^{n}}{\Delta t} - J^{n+1/2} - S^{n+1/2} \right] \quad (9)$$

Clearly Equation 9 cannot be solved directly as each calculation of $\psi n+1$ requires the determination of the coefficients at the mid-interval. Therefore, an iterative solution procedure is necessary. In the current work a predictor-corrector approach is used (Thomas and Rees, 1991). Mathematically, the predictor is expressed as:

$$\psi_p^{n+1} = \left[K_0^{n} + \frac{C_0^{n}}{\Delta t} \right]^{-1} + \left[\frac{C_0^{n}\psi_0^{n}}{\Delta t} - J_0^{n} - S_0^{n} \right] \quad (10)$$

The mid-interval values of ψ are calculated next such that:

$$\psi_1^{n+1/2} = \left(\psi_o^{n} + \psi_p^{n+1} \right) / 2 \quad (11)$$

And the first correction is made as:

$$\psi_{1c}^{n+1} = \left[K_1^{n+1/2} + \frac{C_1^{n+1/2}}{\Delta t} \right]^{-1} + \left[\frac{C_1^{n+1/2}\psi_o^{n}}{\Delta t} - J_1^{n+1/2} - S_1^{n+1/2} \right] \quad (12)$$

In Equation12 the matrices *K*, *C*, *J* and *S* are evaluated corresponding to the values of ψ given in Equation 11. The next correction is made based on a new set of values of $\psi n+1/2$ i.e.:

$$\psi_2^{n+1/2} = \left(\psi_o^{n} + \psi_{1c}^{n+1} \right) / 2 \quad (13)$$

And therefore:

$$\psi_{2c}^{n+1} = \left[K_2^{n+1/2} + \frac{C_2^{n+1/2}}{\Delta t} \right]^{-1} + \left[\frac{C_2^{n+1/2}\psi_o^{n}}{\Delta t} - J_2^{n+1/2} - S_2^{n+1/2} \right] \quad (14)$$

As the process continues the matrices are evaluated at the last mid-interval estimate. Convergence is monitored between successive correctors and is deemed to have been achieved when:

$$\left| \psi_{ic}^{n+1} - \psi_{(i+1)c}^{n+1} \right| < TOLERANCE \quad \text{For all } \psi \quad (15)$$

The value of *TOLERANCE* is judged for the case at hand, throughout the current work and the value adopted is a capillary potential of -1 cm of water.The resulting numerical solution has been coded using FORTRAN.

Evaluation of the numerical model

The mesh consists of 8-noded isoperimetric linear strain quadrilateral elements with 8-displacement and 8-pore pressure nodes placed at the corners of each element (Mu'azu et al., 2011). The entire mesh, Finite Element mesh, consists of 1281 nodes, 400 elements and the overall size of the finite element domain is 10 m × 10 m as shown in Figure 1. Figure 2 shows a diagrammatic representation of the tree, the extent of the root zone (Mu'azu et al., 2011), the root zone is assumed to extend to a depth of 2 m and a

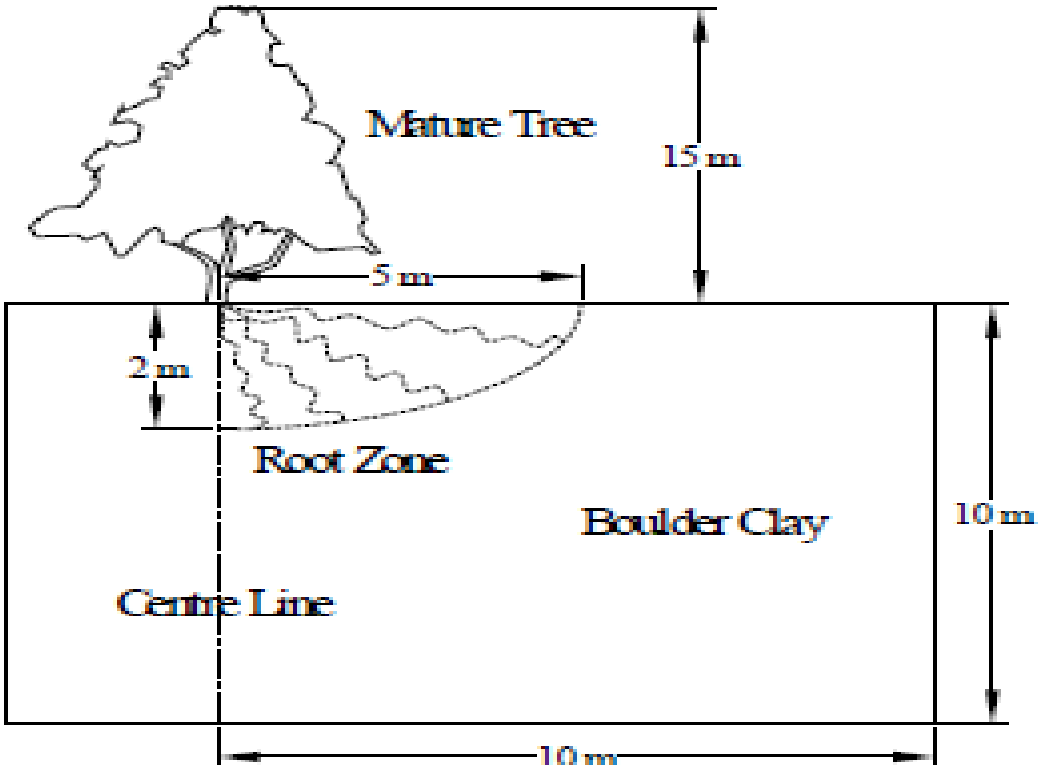

Figure 2. The extent of the root zone.

Table 1. Parameters used in the analysis for simulation.

Parameter	Value	References
ks	10-6 m/s	Lee et al. (1990)
Tp	5 mm/day	Lee et al. (1990)
ψd	1500 kPa	Feddes et al. (1976)
θr	0.1	Rees and Ali (2006)
θs	0.4	Rees and Ali (2006)
α	0.560	Rees and Ali (2006)
m	0.29	Rees and Ali (2006)
n	1.4	Rees and Ali (2006)
l	0.5	Rees and Ali (2006)

radial distance of 5 m. A Lime tree on Boulder Clay was used for the simulation work. A summary of the relevant properties of Boulder Clay soil is shown in Table 1.

RESULTS AND DISCUSSION

A lime tree of 15 m height on Boulder Clay was used in simulation analysis. The initial time step size effects were examined in the overall simulation work, to ensure that the different initial time step sizes simulation results should not differ more than ±5%. The evaluated initial time step sizes are ¼, ½ and 1 day at 0.0, 1.4 and 3.0 m.

Capillary potential for initial time step sizes of ¼, ½ and 1 day at 0.0 m from the lime tree

The initial time step size of ¼, ½ and 1 day were numerically simulated to estimate the capillary potential at the distance of 0.0 m from the Lime tree on Boulder Clay. Therefore, Figures 3 to 6 shows the simulated result of the generated capillary potentials for elapse time of 30, 90, 190 and 270 days at 0.0 m from the trunk of the tree to check the convergence problems. It was discovered that a lower time step size resulted in capillary potential increase and consequently capillary potential increases with an increase in elapsed time.

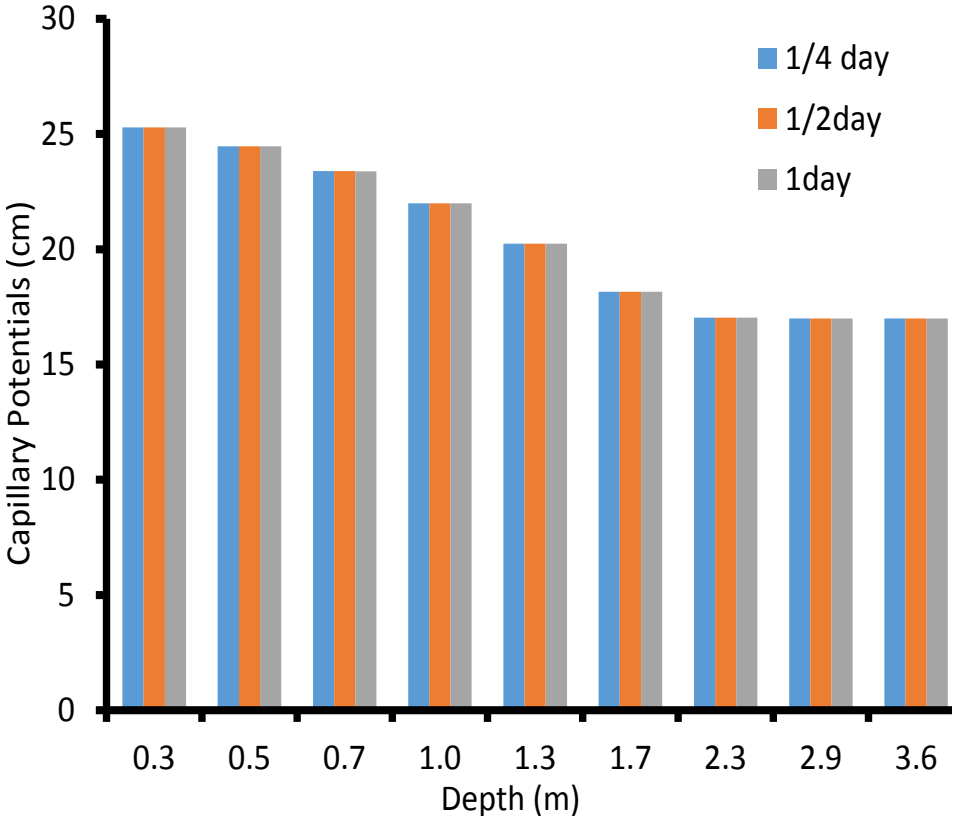

Figure 3. Graph of time step sizes with capillary potential and depth, at 0.0 from the lime tree for 30 days.

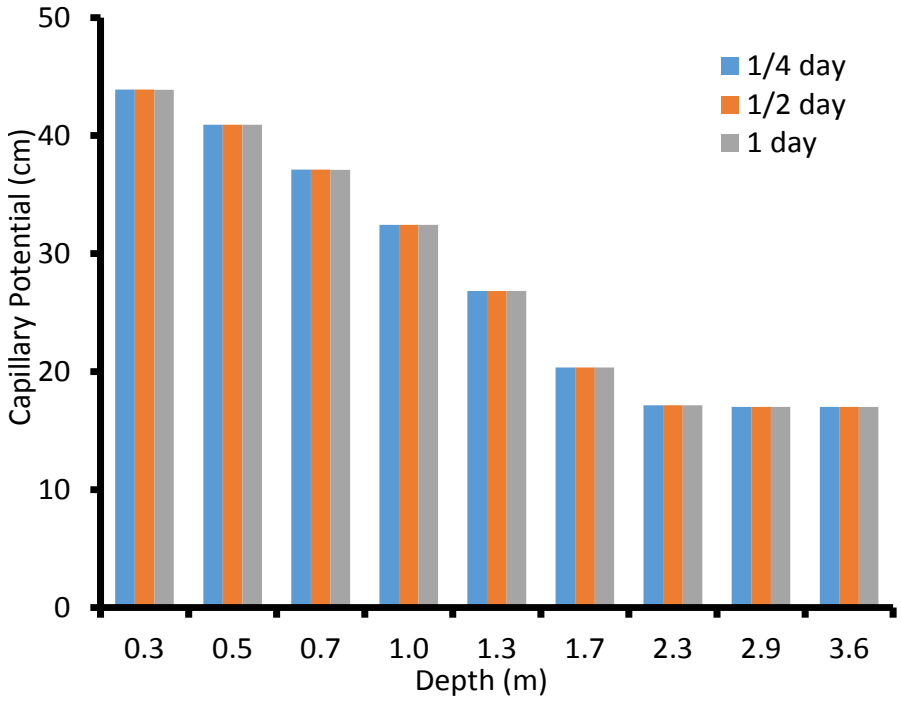

Figure 4. Graph of time step sizes with capillary potential and depth, at 0.0 from the lime tree for 90 days.

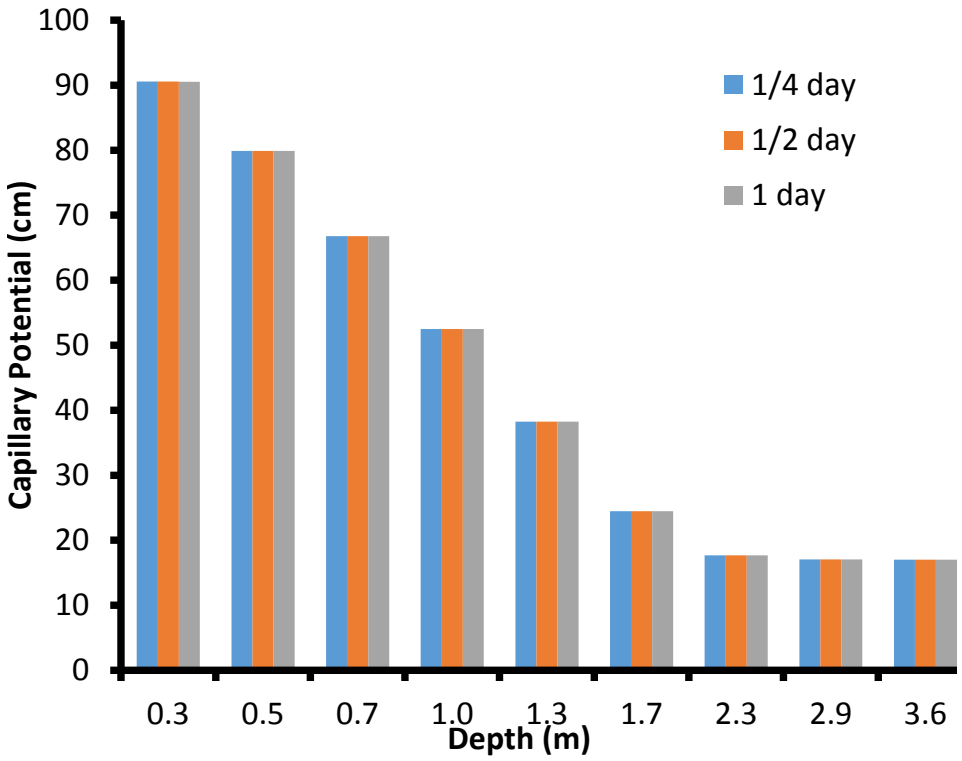

Figure 5. Graph of time step sizes with capillary potential and depth, at 0.0 from the lime tree for 190 days**.**

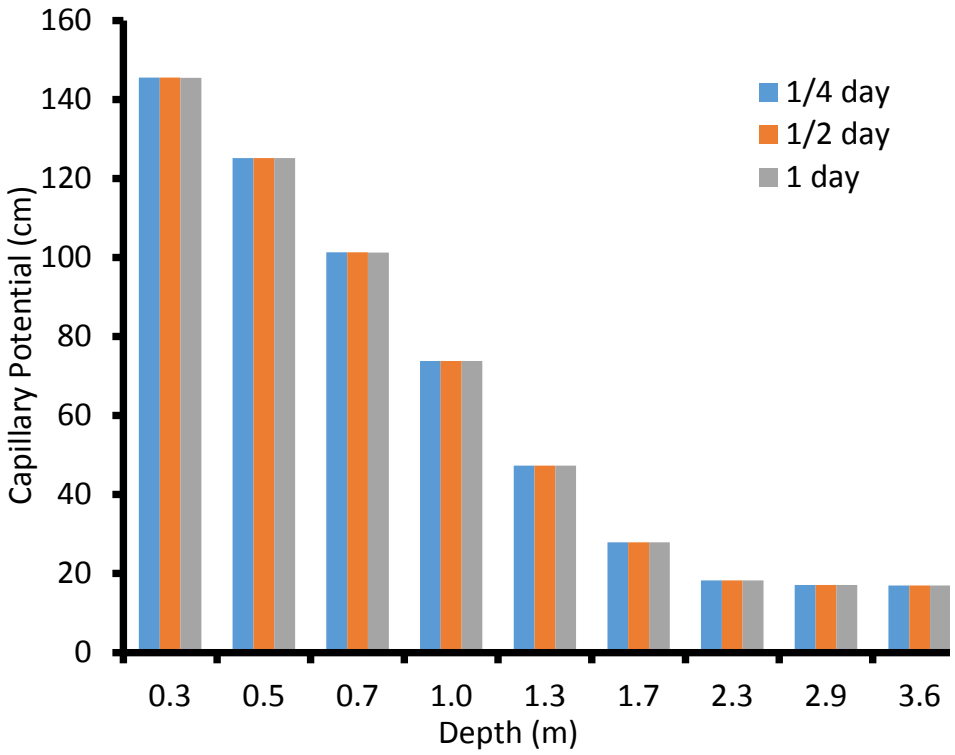

Figure 6. Graph of time step sizes with capillary potential and depth, at 0.0 from the lime tree for 270 days.

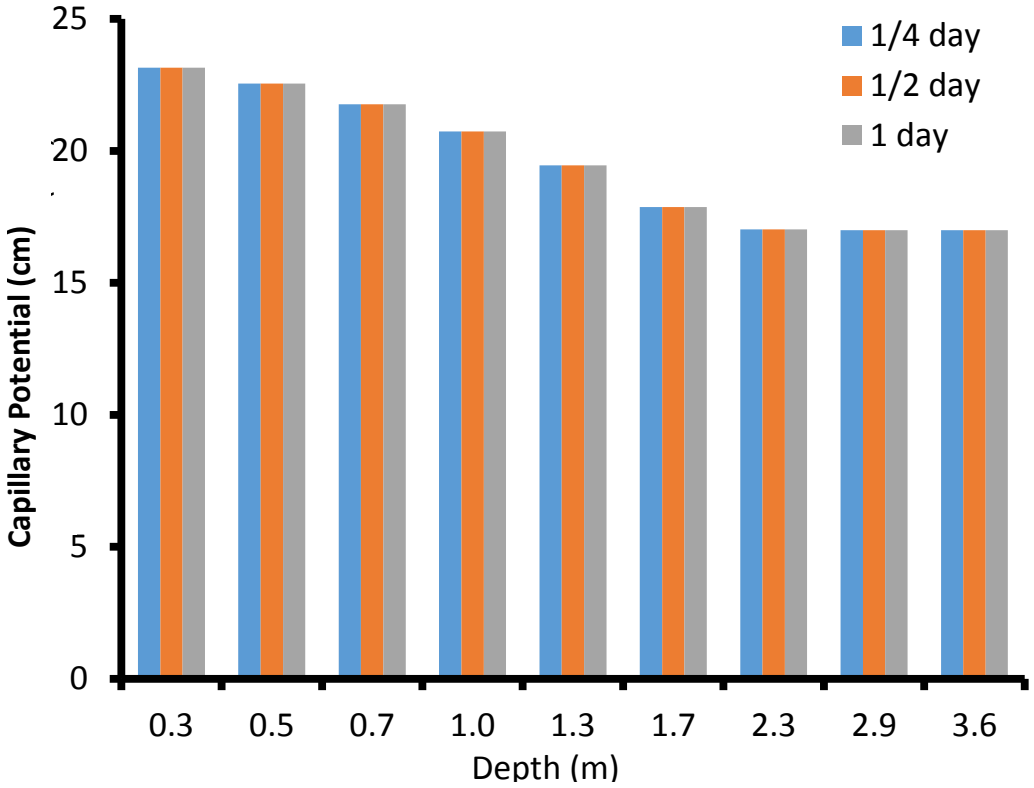

Figure 7. Graph of time step sizes with capillary potential and depth, at 1.4 m from the lime tree after 30 days.

The closer the proximity to the Lime tree also the more the generated capillary potential.

Analysis of the capillary potential generated reveals that the three studied time step sizes at 0.0 m distance, at the same elapsed times generated the same capillary potentials. The spatial distribution of capillary potential at a lower time step is found to produce more realistic simulation capillary potential pattern.

Capillary potential for initial time step sizes of ¼, ½ and 1 day at 1.4 m from the lime tree

The initial time step size of ¼, ½ and 1 day were used in the numerical simulation to estimate the capillary potential for the purpose of the comparison of the initial time step sizes. Figures 7 to 10 shows the generated capillary potential for elapsed time of 30, 90, 190 and 270 days at 1.4 m away from the trunk of the tree. The result is the same sequence as simulation initial time step size of ¼, ½ and 1 day at a distance of 0.0 m from the tree trunk. The only distance is a lower generated capillary potential as a result of increase in lateral distance away from the tree trunk. Lastly, in order to validate the consistency of the effects of change in time step size on the simulation capillary potential, one more simulation was carried out at 3.0 m from the lime tree.

Capillary potential for initial time step sizes of ¼, ½ and 1 day at 3.0 m from the lime tree

The initial time step size of ¼, ½ and 1 day were used in the numerical simulation to estimate the capillary potential to see the effect of initial time step size. Figures 11 to 14 show the simulated result of the generated capillary potential for elapse time of 30, 90, 190 and 270 days at 3.0 m away from the trunk of the tree. Time step sizes were studied with various spacial distances away from the tree trunk at elapsed time of 30, 90, 190 and 270 respectively. The generated capillary potentials was found to be approximated the same as the same spatial distance and elapsed time. Therefore, the choice of the time step size is critical for the efficiency and accuracy of transient simulations (Lee et al., 1990). This check was performed to ensure the assumptions were appropriately made in relation to the time step size and generated capillary potentials. This suggests that accurate selection of time step sizes is crucial for root water-uptake analysis. The initial time step sizes analyzed were found to be satisfactory as the convergence criteria was met.

Conclusion

The simulated capillary potential for time step sizes are

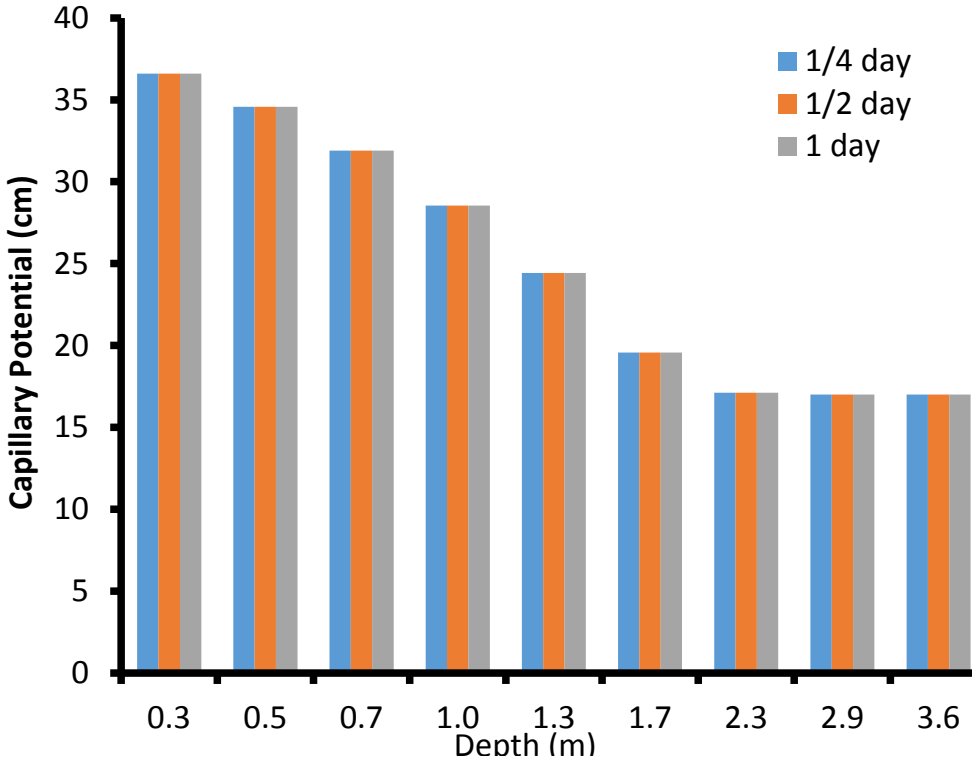

Figure 8. Graph of time step sizes with capillary potential and depth at 1.4 m from the lime tree after 90 days.

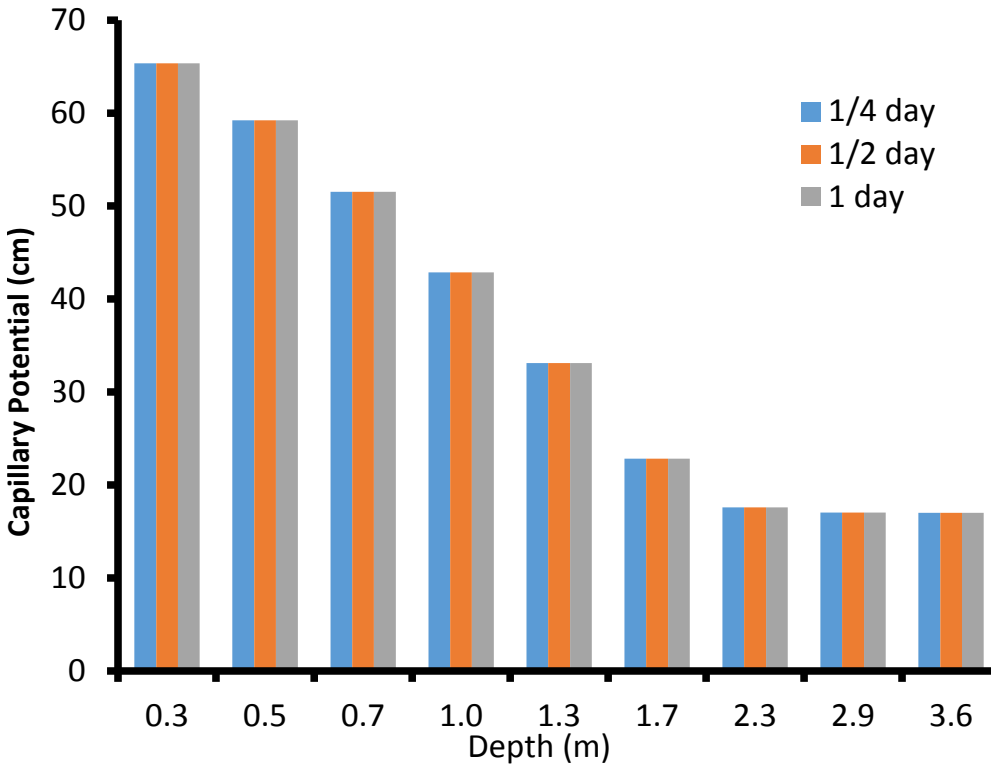

Figure 9. Graph of time step sizes with capillary potential and depth, at 1.4 m from the lime tree after 190 days

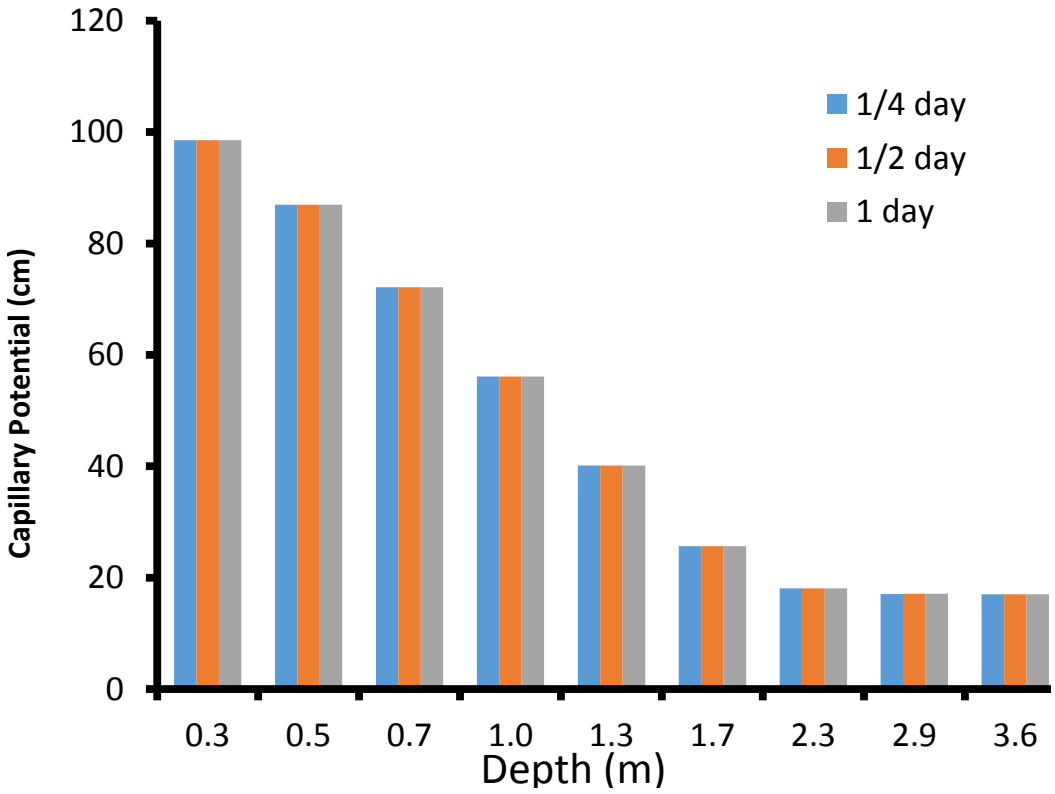

Figure 10. Graph of time step sizes with capillary potential and depth, at 1.4 m from the lime tree after 270 days

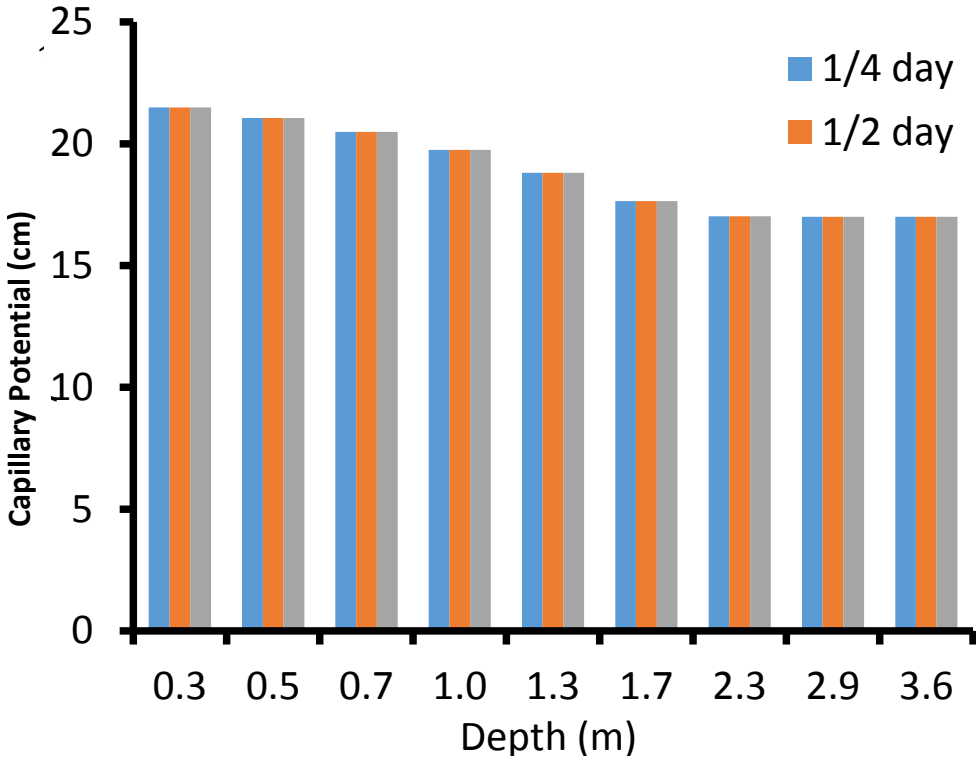

Figure 11. Graph of time step sizes with capillary potential and depth, at 3.0 m from the lime tree after 30 days.

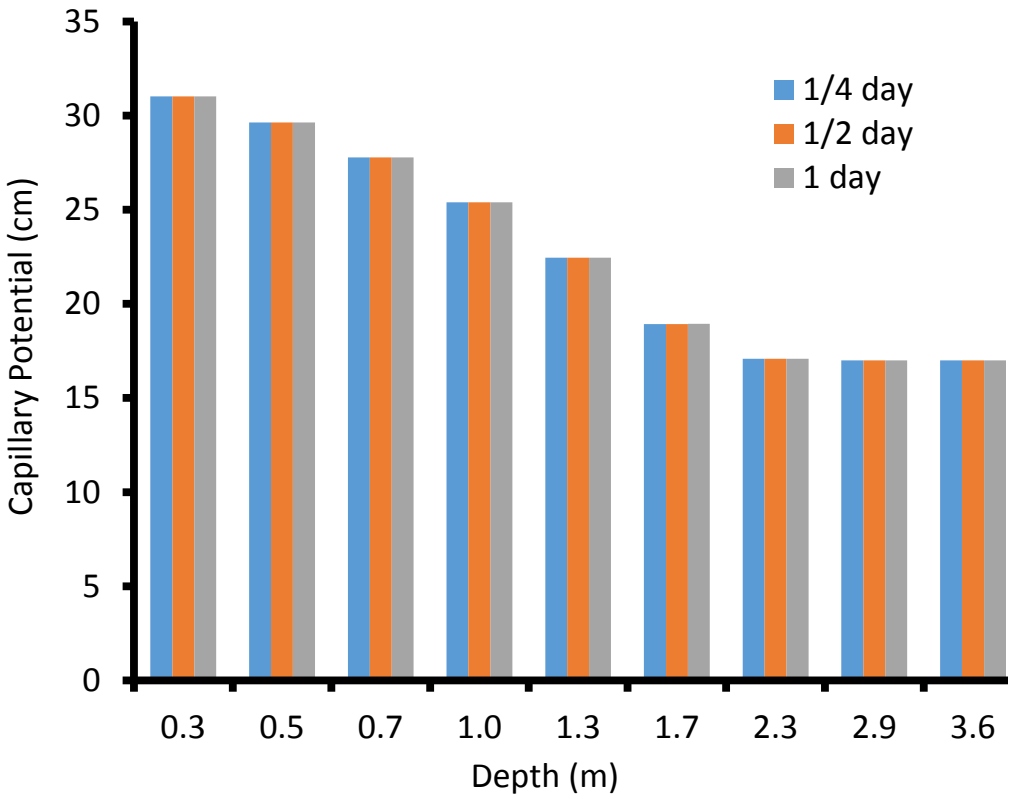

Figure 12. Graph of time step sizes with capillary potential and depth, at 3.0 m from the lime tree after 90 days.

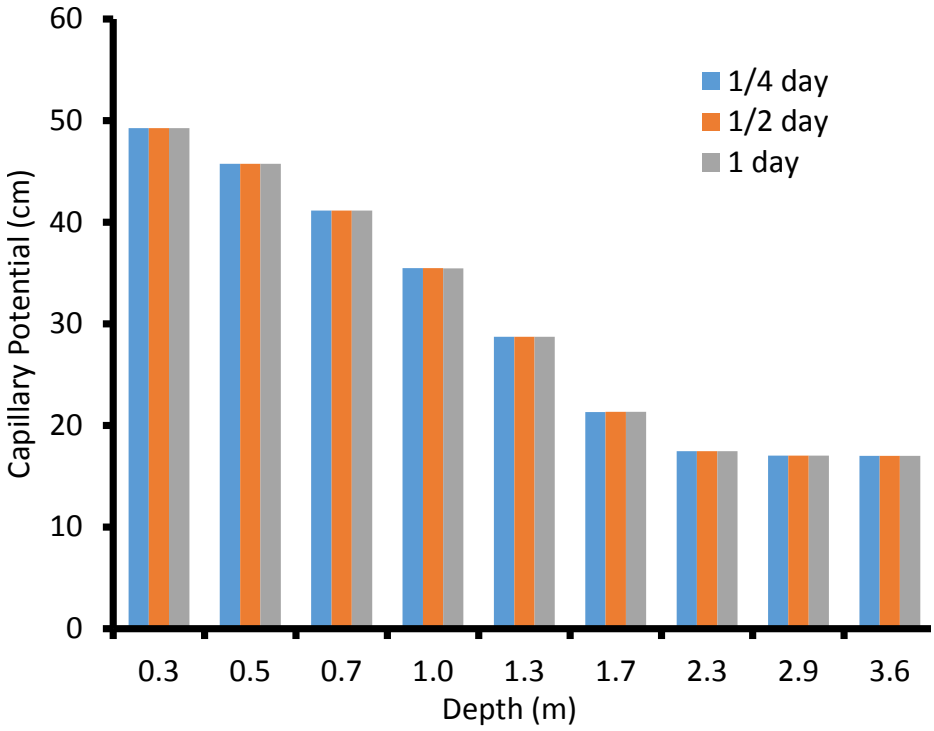

Figure 13. Graph of time step sizes with capillary potential and depth, at 3.0 m from the lime tree after 190 days.

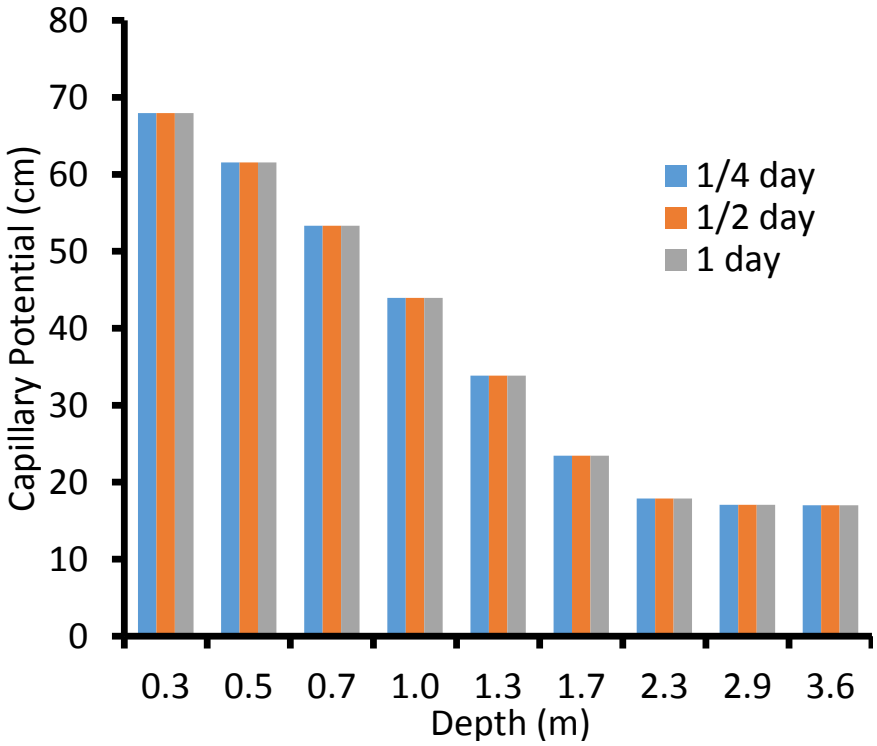

Figure 14. Graph of time step sizes with capillary potential and depth, at 3.0 m from the lime tree after 270 days.

¼, ½ and 1 day at 0.0, 1.4 and 3.0 m away from the lime tree differs not more than ±5%. The ideas is to check whether the simulated results at ¼, ½ and 1 days time steps sizes at same spatial distance from the tree as well as same elapsed time, are the same. The results generated shows that time step sizes investigated have met the convergence criteria. The various time step sizes used in the analysis to test convergence criteria were found to differ by not more than ±5%, which is satisfactory.

CONFLICT OF INTERESTS

The authors has not declared any conflict of interests.

REFERENCES

Alonso EE, Gens A, Hight DW (1987). Special problem soils. Ninth European Conference on Soil Mechanics and Foundation Engineering. Dublin, Ireland, Balkewma, Rotterdam, the Neitherland. 31 August-3 September 3:1087-1146.

Biddle PG (1998). Tree Root Damage to Buildings, Pattern of soil Drying in Proximity to Trees on Clay Soils. 1st Edn., Willow mead Publishing Ltd, Wantage 2:88-93.

Bechmann M, Schneider C, Carminati A, Vetterlein D, Attinger S, Hildebrandt A (2014). Effect of parameter choice in root water uptake models – the arrangement of root hydraulic properties within the root architecture affects dynamics and efficiency of root water uptake. Hydrol. Earth Syst. Sci. 18:4189-4206.

Dai Z, Keating E, Gable C, Levitt D, Heikoop J, Simmons A (2010). Stepwise inversion of a groundwater flow model with multi-scale observation data. Hydrogeol. J. 18:607-624.

Daly KR, Tracy SR, Crout NMJ, Mairhofer S, Pridmore TP, Mooney SJ, Roose T (2017). Quantification of root water uptake in soil using X-ray computed tomography and image-based modeling. Plant, Cell Environ. (doi:10.1111/pce.12983)

Fatahi B, Khabbaz H, Indraratna B (2009). Parametric studies on bioengineering effects of tree root-based suction on ground behavior. Ecol. Eng. 35(10):1415-1426.

Fatahi B, Khabbaz H, Indraratna B (2010). Bioengineering ground improvement considering root water uptake model. Ecol. Eng. 36(2):222-229.

Feddes RA, Kowalik PJ, Malink KK, Zaradny H (1976). Simulation of field water uptake by plants using a soil water dependent root extraction function. J. Hydrol. 31:13-26.

Fredlund DG, Hung VQ (2001). Predictive of volume change in an expansive soil as a result of vegetation and environmental changes. Pro. of ASCE Conf. on expansive clay soils and vegetative influence on shallow foundations, Geotechnical Special Publication. Houston, Texas, Reston, USA. 10-13 October. pp. 24-43.

Lee SH, Steve S.Hsieh SS (1990). Expedient implicit integration with adaptive time stepping algorithm for nonlinear transient analysis. Comput. Methods Appl. Mech. Eng. 81(2):151-172.

Kumar R, Shankar V, Jat MK (2014). Evaluation of root water uptake models-a review. ISH J. Hydraulic Eng. 21(2):1-10.

Li L, van der CT, Chen X, Jing C, Su B, Luo G, Tian X (2013). Representing the root water uptake process in the Common Land Model for better simulating the energy and water vapour fluxes in a Central Asian desert ecosystem. J. Hydrol. 502:145-155.

Liao R, Yang P, Wu W, Ren S (2016). An Inverse Method to Estimate the Root Water Uptake Source-Sink Term in Soil Water Transport Equation under the Effect of Superabsorbent Polymer, PLoS ONE 11(8):e0159936.

Mathur S, Rao S (1999). Modeling water uptake by plant roots. J. Irrig.

Drainage Eng. 125(3):159-165.
Mu'azu MA, Nazri A, Kamarudin A (2011). Vegetative induced ground displacements: a comparison of numerical and experimental study. Sci. Res. Essays 6(27):5757-5770.
Mohsen Z, Eva K, Anders K, Andrea C (2014). Visualization of Root Water Uptake: Quantification of Deuterated Water Transport in Roots Using Neutron Radiography and Numerical Modeling[C]. Plant Physiol. 166:487-499.
Martin G, Petra L-B, Felicitas S, Christopher POR (2015). Modeling of Two Different Water Uptake Approaches for Mono- and Mixed-Species Forest Stands. For. 6:2125-2147.
Navarro V, Candel M, Yustres A, Sanchez J, Alonso J (2009). Trees, soil movement and foundation. Comput. Geotech. 36(5):810-818.
Neuman SP (1973). Saturated-unsaturated seepage by finite elements. Proceedings of the Hydraulics Division. ASCE 99(12):2233-2250.
Nyambayo VP, Potts DM (2010). Numerical simulation of evapotranspiration using a root water uptake model. Comput. Geotech. 37(3):175-186.
Philip JR (1957). The theory of infiltration 1: The infiltration equation and its solution. Soil Sci. 83(5):345-357.
Rees SW, Ali N (2006). Seasonal water uptake near trees: A numerical and experimental study. Geomech. Geo-Eng. 1(2):129-138.
Richards LA (1931). Capillary conductance of liquids through porous mediums. J. Appl. Phys. 1:318-333.
Rockey KC, Evans HR, Griffiths DW, Nethercot DA (1983). The Finite Element Method. London: Collins. 2nd Edn.
Saroj KM, Sandeep S (2011). Effects of time step size on the simulation of the tropical climate in NCAR-CAM3. Clim. Dyn. 37:689-704.
Teixeira J, Reynolds CA, Judd K (2007). Time step Sensitivity of Nonlinear Atmospheric Models: Numerical Convergence, Truncation Error Growth, and Ensemble Design. J. Atmos. Sci. 64:175-189.
Thomas HR, Rees SW (1991). A comparison of field monitored and numerically predicted moisture movement in unsaturated soil. Int. J. Num. Anal. Methods Geomech. 15(6):417-431.
Tsutomu Y, Takeo K, Xinchao S, Hiroaki K, Yuichi O (2017). Comparing root water uptake profile estimations from an isotope-calibrated mechanistic model and a mixing model. Hydrol. Res. Lett. 11(3):161-167.
Zienkiewicz OC, Taylor RL (1989). The Finite Element Method. 4th Edn., Vol. 1, McGraw-Hill,USA. P 648.